Exploring the influence of three-body classical dispersion forces on phase equilibria of simple fluids: An integral-equation approach

J. A. Anta, E. Lomba, and M. Lombardero
Instituto de Química Física Rocasolano, Consejo Superior de Investigaciones Científicas, Serrano 119, E-28006 Madrid, Spain
and Departamento de Química Física I, Universidad Complutense, E-28040 Madrid, Spain
(Received 23 June 1993)

We investigate a recently introduced integral equation which takes into account three-body interactions via an effective pair potential. The scheme proposed here essentially reduces to solving a reference hypernetted-chain equation with a state-dependent effective potential, and a hard-sphere reference bridge function that minimizes the free energy per particle. Our computational algorithm is shown to be stable and rapidly convergent. As a whole, the proposed procedure yields thermodynamic properties in accordance with simulation results for systems with Axilrod-Teller triple-dipole potential plus a Lennard-Jones interaction, and improves upon previous integral-equation calculations. Predictions obtained for the gas-liquid coexistence of argon are in remarkable agreement with experimental results, and show unequivocally that the influence of the three-body classical dispersion forces (and not only quantum effects) must be explicitly incorporated to account for the deviations between pure Lennard-Jones systems and real fluids. Moreover, the integral equation approach as introduced here proves to be a reliable tool and an inexpensive probe to assess the influence of three-body interactions in a consistent way. For completeness, the no-solution line of the integral equation is also presented. A study of the behavior of the isothermal compressibility in the vicinity of the no-solution boundary shows the presence of a divergence that deviates from a power law at high densities, and the appearance of a singularity with the characteristics of square-root branch point at low density (a feature also found in the hypernetted-chain approximation in a variety of systems). The no-solution line, unfortunately, hides the coexistence curve near the critical point, and this constitutes the only severe drawback in our approach. An alternative for bypassing this shortcoming is explored.

PACS number(s): 61.20.Gy, 61.25.Bi, 64.60.Fr, 64.70.Fx

I. INTRODUCTION

In the standard statistical-mechanics treatment of fluids, the principle of pairwise additivity of the potential energy is widely assumed to be valid. However, already in the early seventies, Barker and co-workers [1–4] showed unambiguously that a three-body interaction (the Axilrod-Teller [5] triple-dipole potential) had to be incorporated to correctly describe the experimental properties of argon. Recently, Attard [6] has shown that the perturbation approach proposed by Barker *et al.* is virtually exact for argon, both in the gas and liquid regimes. Nevertheless, the integral-equation approach proposed by Attard [7] is extremely attractive in its own, even if it cannot match at high densities the perturbation theory. Attard's reduction of the three-body problem via the introduction of a state-dependent effective pair potential is a conceptually simple path of introducing the effect of three-body correlations in the powerful integral-equation theory for pairwise additive potentials. As a matter of fact, the effective-potential route was first explored by Rushbrooke and Silbert [8] and Casanova *et al.* [9] in the late sixties, in a somewhat simpler treatment. We will here explore a modest improvement of Attard's extension of the reference hypernetted-chain (RHNC) closure [6] by introducing a consistent criterion for the definition of the reference system. In this respect, our choice has been the free-energy minimization proposed by Lado, Foiles, and Ashcroft [10] which is computationally less involved than the requirement of thermodynamic consistency between virial and isothermal compressibility routes. In particular, we will consider again argon as a testing ground for the proposed theoretical scheme, focusing on its phase coexistence properties.

The purpose of the present work is thus twofold. On the one hand, we want to analyze the ability of the optimized integral equation for the prediction of experimental results in systems with three-body interactions. We will see that integral-equation results are remarkably good, although they do not match the perturbative approach. The optimized RHNC equation with effective interaction is thus found to be a powerful tool of predicting thermodynamic properties in real systems. On the other hand, we have explored the sensitivity of thermodynamic properties and, in particular, the coexistence curve to the introduction of three-body classical dispersion forces. We find that by taking into account these interactions brings the integral-equation results to a much closer agreement with the experimental gas-liquid coexistence curves. This makes it evident that the effects of the polarizability are crucial when studying chemical equilibrium. In relation with this, in an earlier work, Hansen and Verlet [11] attributed the disagreement on the gas side of the coexistence curve between Lennard-Jones (LJ) fluid models and

experimental results to the well known failure of the LJ potential for argon at low densities and low temperatures [12]. We will see that the improvement on the low-density side of the coexistence curve reflects (through the chemical equilibrium condition) a more appropriate treatment of its liquid counterpart by incorporating three-body effects, that are obviously more important at high densities.

This paper can be sketched as follows. Section II is devoted to a brief summary of the theory. In Sec. III thermodynamic properties computed in the optimized RHNC approximation are analyzed and compared with Monte Carlo data, and previous RHNC and perturbation theory calculations. Here we illustrate how the introduction of an optimization criterion to define the reference system improves the thermodynamic results. A theoretical estimate for the phase diagram of Ar is determined by applying chemical equilibrium conditions. Finally, in Section IV we present a study of the "critical" behavior of the integral equation both in the low-density and high-density boundaries of its no-solution region. Our analysis shows that there is a region of physical significance in the neighborhood of the critical point which is unreachable to the RHNC equation. In this respect, a preliminary calculation [13] for the two-body system using the crossover closure relation (CRS) [14] shows that this equation might be an alternative to bypass the deficiencies of the RHNC in that region (and, in general, to cope with the failure of the HNC to yield and appropriate spinodal behavior at low densities [15,16]. However, this latter approach lacks an important and desirable feature present in other approximations, namely, the availability of a closed expression to compute chemical potentials from correlation functions.

II. THEORY

A. Model potential

Particles in a 6-12 Lennard-Jones (LJ) fluid interact via a pair potential of the form

$$u^{(2)}(r) = 4\epsilon\left[(\sigma/r)^{12} - (\sigma/r)^{6}\right]. \tag{1}$$

In addition to the plain pair interaction we will here introduce the Axilrod-Teller three-body potential [5]

$$u^{(3)}(\mathbf{r}_1,\mathbf{r}_2,\mathbf{r}_3) = \nu\frac{r_{12}^2 r_{13}^2 r_{23}^2 + 3(\mathbf{r}_{12}\cdot\mathbf{r}_{13})(\mathbf{r}_{21}\cdot\mathbf{r}_{23})(\mathbf{r}_{31}\cdot\mathbf{r}_{23})}{r_{12}^5 r_{13}^5 r_{23}^5}. \tag{2}$$

Thus, the full N-particle potential energy to be considered reads

$$U_N = \sum_{\substack{i,j\\ i<j}}^{N} u^{(2)}(r_{ij}) + \sum_{\substack{i,j,k\\ i<j<k}}^{N} u^{(3)}(\mathbf{r}_i,\mathbf{r}_j,\mathbf{r}_k). \tag{3}$$

The net effect of this potential energy could be expressed in terms of two-body functions if an effective *pair* potential that accounts for the three-body interactions can be defined. This has recently been done in an elegant way by Attard [7], who introduced the following effective pair interaction:

$$\beta u^{\mathrm{eff}}(r_{12}) = -\rho\int[e^{-\beta u^{(3)}(\mathbf{r}_1,\mathbf{r}_2,\mathbf{r}_3)} - 1]g(r_{13})g(r_{32})d\mathbf{r}_3. \tag{4}$$

As formulated in Eq. (4), $\beta u^{\mathrm{eff}}(r_{12})$ is a functional of the pair distribution function, i.e., it is a state-dependent quantity, which, as Attard has shown [7], retains the leading contribution of three-body interactions to the pair potential of mean force.

B. The Ornstein-Zernike equation and RHNC closure

For homogeneous simple fluids the Ornstein-Zernike relation reads

$$\gamma(r_{12}) = \rho\int c(r_{32})\left[\gamma(r_{13}) + h(r_{13})\right]d\mathbf{r}_{13}\ , \tag{5}$$

where c is the direct correlation function and $\gamma = h - c$ is the series function [17]. This equation is closed by a functional relation between c and γ, that is usually written

$$c(r_{12}) = \exp\left[-\beta u^{(2)}(r_{12}) + \gamma(r_{12}) - B(r_{12})\right] - \gamma(r_{12}) - 1\ , \tag{6}$$

where B is the bridge function. In the RHNC one assumes

$$B(r_{12}) = B_0(r_{12}) \tag{7}$$

with B_0 being the bridge function of a reference system. In simple fluids the hard-sphere fluid constitutes the simplest and best suited choice. In this case one must find a consistent criterion to define the single parameter that determines all properties (including the bridge function) of the reference system, that is the hard-core diameter. Lado, Foiles, and Ashcroft [10] gave a physically sound answer to this question for pairwise additive systems, and we will see in the next subsection how their explicit recipe can be applied in the context of this work as well.

The hard-sphere bridge function can be easily evaluated via the empirical formula proposed by Labik and Malijevsky [18], which has shown to render excellent results in the context of RHNC calculations for simple LJ fluids [19] and is the approach adopted in this work.

Following Attard, in the present instance, the RHNC closure relation (6) has the form

$$c(r_{12}) = \exp[\ -\beta u^{(2)}(r_{12}) - \beta u^{\mathrm{eff}}(r_{12}) + \gamma(r_{12}) - B_0(r_{12})] - \gamma(r_{12}) - 1\ , \tag{8}$$

where $u^{\mathrm{eff}}(r)$ is given by Eq. (4). Since the effective pair potential is a convolution of the pair distribution function, the closure is no longer a local functional of $\gamma(r)$ and the solution procedure becomes more involved. Equations (5), (7), and (8) form a closed system of equations which can be solved by successive iterations. We here propose the use of a hybrid Newton-Raphson iterative

scheme [20, 19] which considerably accelerates convergence and is particularly adequate for the present problem.

C. Three-body integrals and thermodynamic quantities: Optimized RHNC closure

When the N-particle potential energy of the system is given by Eq. (3) three-body contributions must be added to the usual thermodynamic relations. These contributions are integrals involving the triplet distribution function $g^{(3)}$, that can be estimated using an extension of the well known Kirkwood superposition approximation [21], in which an exponential term is added to account for the explicit presence of a three-body interaction [6, 7, 22], namely

$$g^{(3)}(\mathbf{r}_1,\mathbf{r}_2,\mathbf{r}_3)= g(\mathbf{r}_1,\mathbf{r}_2)g(\mathbf{r}_1,\mathbf{r}_3)g(\mathbf{r}_2,\mathbf{r}_3)e^{-\beta u^{(3)}(\mathbf{r}_1,\mathbf{r}_2,\mathbf{r}_3)} . \tag{9}$$

By defining a coordinate system with the origin at particle 1, and the z axis placed along the vector joining particles 1 and 2, the set of variables required to describe a three-particle configuration reduces to $\{r_{12}, r_{13}, x\}$ where $x = \mathbf{r}_{12}\cdot\mathbf{r}_{13}/r_{12}r_{13}$. The effective potential then reads

$$\beta u^{\rm eff}(r_{12}) = -2\pi\rho\int_{-1}^{1}\int_{0}^{\infty}\left[e^{-\beta u^{(3)}(r_{12},r_{13},x)}-1\right] \times g(r_{13})g(\sqrt{r_{12}^2+r_{13}^2-2r_{12}r_{13}x}) \times r_{13}^2 dr_{13}dx \tag{10}$$

and the Axilrod-Teller interaction

$$u^{(3)}(r_{12},r_{13},x) = \nu\frac{r_{12}^2+r_{13}^2+r_{12}r_{13}x-3r_{12}^2x^2-3r_{13}^2x^2+3r_{12}r_{13}x^3}{r_{12}^3r_{13}^3(r_{12}^2+r_{13}^2-2r_{12}r_{13}x)^{\frac{5}{2}}} . \tag{11}$$

Hence, the following relations for the excess energy and pressure can be derived:

$$\frac{\beta U^{\rm ex}}{N} = 2\pi\rho\int_0^\infty u^{(2)}(r_{12})g(r_{12})r_{12}^2dr_{12} + \frac{4\pi^2\rho^2}{3}\int_0^\infty\int_0^\infty\int_{-1}^{1}\beta u^{(3)}(r_{12},r_{13},x)g^{(3)}(r_{12},r_{13},x)r_{12}^2r_{13}^2dr_{12}dr_{13}dx , \tag{12}$$

$$\frac{\beta P}{\rho} = 1-\frac{2\pi\rho}{3}\int_0^\infty\beta r_{12}^3\frac{\partial u^{(2)}(r_{12})}{\partial r_{12}}dr_{12} - \frac{4\pi^2\rho^2}{9}\int_0^\infty\int_0^\infty\int_{-1}^{1}\beta r_{12}^3\frac{\partial u^{(3)}(r_{12},r_{13},x)}{\partial r_{12}}g^{(3)}(r_{12},r_{13},x)r_{12}^2r_{13}^2dr_{12}dr_{13}dx. \tag{13}$$

In order to build the phase diagram we need an expression to evaluate the three-body contribution to the excess free energy. Attard [7] derived an appropriate formula that in our variables reads

$$\frac{\beta A^{(3)}}{N} = \frac{8\pi^2\rho^2}{3}\int_0^\infty\int_0^\infty\int_{-1}^{1}\left[e^{-\beta u^{(3)}(r_{12},r_{13},x)}-1\right]g^{(3)}(r_{12},r_{13},x)r_{12}^2r_{13}^2dr_{12}dr_{13}dx \tag{14}$$

to which, in our case, the standard RHNC free energy for pairwise additive systems is added [10]

$$\frac{\beta A^{(2)}}{N} = 2\pi\rho\int_0^\infty r^2g_0(r)B_0(r)dr + \frac{1}{2}\rho\left(\beta/\rho\chi_t-1\right) -\frac{1}{4\pi^2\rho}\int_0^\infty\left\{\rho^2\tilde{h}(k)\left(\frac{1}{2}\tilde{h}(k)-\tilde{\gamma}(k)\right)+\ln\left(1-\rho\tilde{h}(k)\right)-\rho\tilde{h}(k)\right\}k^2dk . \tag{15}$$

In the expression above, g_0 is the reference-system pair distribution function, and χ_T is the isothermal compressibility, as given by

$$\beta/\rho\chi_T = 1-\rho\tilde{c}(0) . \tag{16}$$

Then one simply gets

$$\frac{\beta A^{\rm ex}}{N} = \frac{\beta A^{(2)}}{N}+\frac{\beta A^{(3)}}{N} . \tag{17}$$

As mentioned before, Lado, Foiles, and Ashcroft [10] proposed an optimization criterion to define the reference system so that the Helmholtz free energy is minimized. The reference hard-sphere diameter is determined by requiring that the following condition is fulfilled:

$$4\pi\int_0^\infty\left(g(r)-g_0(r;d)\right)\frac{\partial B_0(r;d)}{\partial d}r^2dr = 0 . \tag{18}$$

This can be shown to lead to a minimum in the free energy [10].

Although Eqs. (15) and (18) are exact in the RHNC scheme for pairwise additive potentials, two conditions must be satisfied for them to be valid when a state-dependent effective potential is incorporated. First, the effective pair potential should be insensitive to variations in the reference hard-sphere system diameter d. This guarantees that the expressions for the two-body contribution to the Helmholtz free energy from the RHNC theory apply in this instance as well. Figure 1 shows the effective pair potential evaluated for two distinct values of d. One readily appreciates that d hardly plays any role in the determination of $u^{\rm eff}$. On the other hand, we need to ensure that the optimization criterion from Eq. (18) (which is also derived in the context of two-body potentials) renders a hard-sphere diameter for which the free energy including three-body contributions reaches a minimum. To see this, in Fig. 2 we have plot-

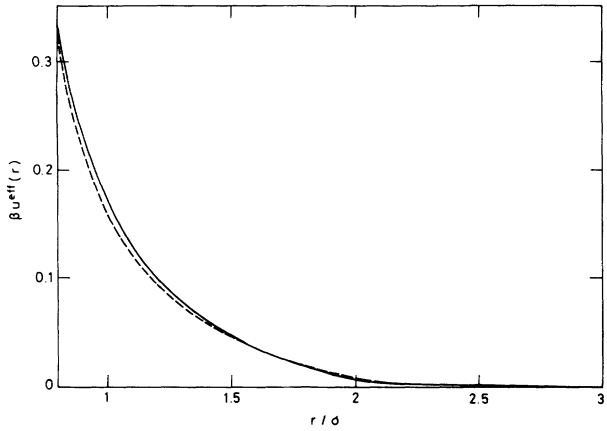

FIG. 1. Effective pair potential from Eq. (4) at $kT/\epsilon = 1.0$ and $\rho\sigma^3 = 0.8$, for $d/\sigma = 1.0$ (solid line) and $d/\sigma = 1.1$ (dashed line), where d is the reference-system hard-sphere diameter.

ted the excess Helmholtz free energy as a function of the reference-system diameter and the value of d which satisfies Eq. (18) is indicated with a filled circle. We see that this value is slightly off the real minimum (by 2%). However, this hardly affects thermodynamic properties, with a maximum deviation in the virial pressure below 1% (internal and free energy are off by less than 0.1%). From these considerations we might conclude that the extension of the optimization procedure to this effective-potential problem is legitimate.

III. THERMODYNAMICS AND PHASE COEXISTENCE

The set of equations formed by Eq. (5) and the closure (8) is solved by use of the hybrid Newton-Raphson procedure proposed by Labík, Malijevsky, and Vonka [20] with the Jacobian matrix remaining constant through the optimization iterations [19].

The essential change with respect to the two-body problem treated in Refs. [19] and [20] lies in the fact that the leading term in the Jacobian $\partial g(r)/\partial\gamma$ is no longer equal to $g(r)$ (as in the case of the two-body HNC and RHNC), but it is slightly more involved due to the functional dependence of βu^{eff} on the pair distribution function. Here, by functional differentiation and retaining only terms linear in $g(r)$ one gets,

$$\frac{\partial g(r_{12})}{\partial\gamma(r_{12})} = g(r_{12})[1 - 2\beta u^{\text{eff}}(r_{12})] \; . \tag{19}$$

One of the main advantages of this method is, in this case, connected with the fact that the core of the iterative scheme (the Newton-Rapshon loop) is carried entirely in Fourier space, and thus the number of closure-relation evaluations (the most time-consuming task) is performed very few times before convergence is achieved. Hence, the proposed method outperforms hybrid procedures like that of Gillan [23] which require one evaluation of the closure per Newton-Raphson iteration, let alone the classical direct-substitution or mixing-iterates methods.

In most of the calculations herein, standard LJ potential parameters for Ar have been used [24], namely, $\epsilon/k = 120$ K, $\sigma = 3.405$ Å , and $\nu/\epsilon\sigma^9 = 0.072$.

As a check of our method in Table I and Fig. 3 we compare results from simulation, previous RHNC calculations [6], and perturbation theory [4], with those obtained by use of the optimized RHNC. Calculations were carried out using 4096 grid points and a grid size $\Delta r = 0.01\sigma$. Three-dimensional integrals in Eqs. (10), (12), (13), and (14) were evaluated using Gauss-Legendre's integration with 80 nodes, and Simpson's rule over the radial coordinate with 200 points. The minimization condition was considered satisfied when the absolute value of the expression (18) was smaller than 10^{-5}. This can be a crucial choice in the neighborhood of the no-solution line.

Results of Table I and Fig. 3 make evident that

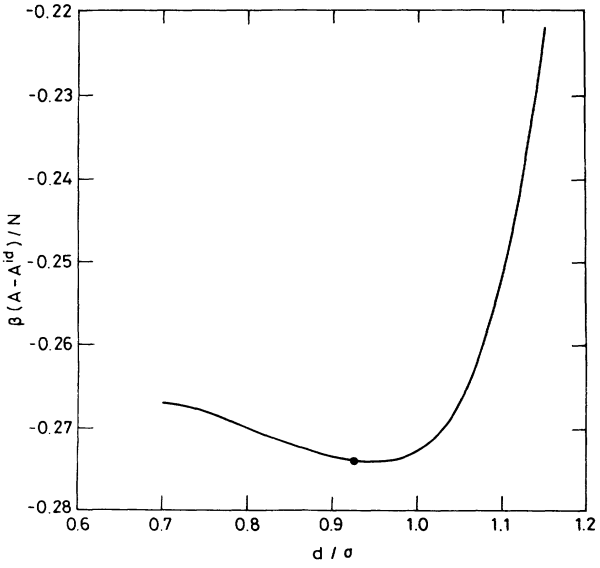

FIG. 2. Excess free energy as a function of the reference-system hard-sphere diameter d. The solid circle indicates the value of d which satisfies Eq. (18).

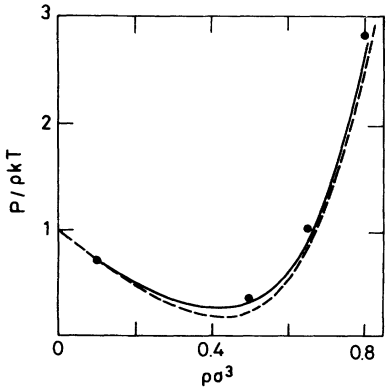

FIG. 3. Compressibility factor of the LJ-Axilrod-Teller fluid at $kT/\epsilon = 1.333$. Solid circles denote MC data, RHNC results with reference-system optimization are represented by a solid line, and a dashed line denotes RHNC results without optimization taken from Ref. [6].

TABLE I. Pressure and internal energy of a fluid whose particles interact thorough a 6-12 LJ potential ($\epsilon/k = 120K$, $\sigma = 3.405$ Å) and the Axilrod-Teller triple-dipole potential ($\nu/\epsilon\sigma^9 = 0.072$) computed via Monte Carlo simulation [6], RHNC approximation [6], perturbation theory [4], and optimized RHNC approximation (present work).

	$kT/\epsilon = 1.033$, $\rho\sigma^3 = 0.65$		$kT/\epsilon = 0.746$, $\rho\sigma^3 = 0.817$	
	U/NkT	$P/\rho kT$	U/NkT	$P/\rho kT$
MC	-4.227	0.15	-7.566	0.56
RHNC	-4.2181	-0.0253	-7.486	0.8054
Pert.	-4.224	0.138	-7.555	0.62
RHNC (op.)	-4.221	-0.049	-7.531	0.241

the optimization procedure somewhat improves previous RHNC calculations. This effect is more visible in the case of the virial pressure where the optimized integral equation brings the theoretical values to a much closer agreement with those obtained from Monte Carlo simulations, as can be seen in Fig. 3. Still, one must note that there is more room for further corrections to be added, and Barker's *et al.* perturbation theory remains unmatched. The problem might actually be now the treatment of the three-body interaction via the effective potential (10). Note in this regard that in the derivation of Eq. (10) an important number of cluster diagrams at least of order ρ^2 are neglected [6], though some are indirectly accounted for through the reference bridge function. Therefore as density approaches the melting point one should not expect Eq. (10) to represent the effective interaction adequately.

When calculations along several isotherms are performed one immediately finds pairs of ρ values (ρ_g, ρ_l) which fulfill the phase equilibrium conditions

$$\beta\mu(\rho_l, T)/N = \beta\mu(\rho_g, T)/N \ , \tag{20}$$
$$\beta P(\rho_l, T)\sigma^3 = \beta P(\rho_g, T)\sigma^3 \ ,$$

where P is the pressure and μ is the chemical potential. This latter quantity is here evaluated through

$$\beta\mu/N = \ln\rho + A^{\rm ex}/NkT + P/\rho kT + f(T) \ , \tag{21}$$

where $f(T)$ is a function of the temperature irrelevant in a isothermal construction. Solving Eqs. (20) we have determined the phase diagram presented in Fig. 4. Inside the no-solution region, the behavior of the coexistence curve was estimated by interpolation and is represented in the figure by a dashed line. In Fig. 4 we also show experimental results for argon [25], simulation values obtained for a 6-12 LJ fluid [26], and the no-solution boundary of the integral equation. We can see that the agreement between three-body RHNC results and experimental data is very satisfactory, especially when comparing with the LJ simulation data. This proves that the three-body classical dispersion forces described by the Axilrod-Teller potential play an important role in phase equilibrium. Explicit results for the phase coexistence are also given in Table II.

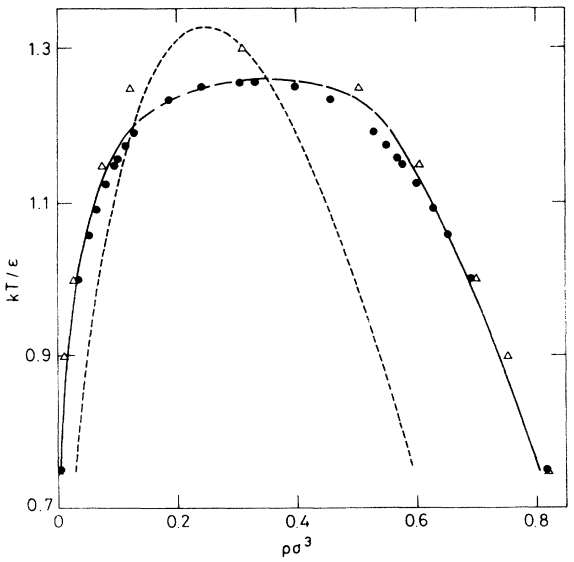

FIG. 4. Gas-liquid phase coexistence for the LJ-Axilrod-Teller fluid. Optimized RHNC theory (solid line), experimental results from Ref. [25] (solid circles), and LJ results from Ref. [26] (open triangles) are represented. The long dashed line corresponds to a rough interpolation. The short-dashed line denotes the no-solution boundary of the RHNC integral equation.

One can see that the agreement is far better on the gas side of the coexistence curve. In relation with this Hansen and Verlet [11] suggested that the well known poor performance of the LJ pair potential for Ar at low ρ and T [12] might be responsible for the deviations between the experimental results and the Lennard-Jones coexistence curve. We have found that the introduction of three-body classical effects does not improve the predictions for the second virial coefficients in the gas phase when compared with the exact Lennard-Jones $B(T)$. This implies that the improvement on the gas phase coexistence curve simply reflects a more appropriate treatment of the liquid side through the equilibrium conditions.

The critical temperature predicted by the theory ($\sim$ 150 K) is quite close to the experimental value of 150.87 K, and is substantially better than the two-body Lennard-Jones fluid critical temperature (163 K). Unfortunately, calculations cannot be extended to the vicinity of the critical region since the numerical solution of the integral equation breaks down. In the next section we investigate the nature of the divergence and possible alternatives to overcome this pitfall.

TABLE II. Phase coexistence data for Argon. LJ results are taken from Ref. [26] and experimental results from Refs. [11] and [25].

	6-12 LJ (sim.)		RHNC(op.)		Expt.	
kT/ϵ	$\rho_g\sigma^3$	$\rho_l\sigma^3$	$\rho_g\sigma^3$	$\rho_l\sigma^3$	$\rho_g\sigma^3$	$\rho_l\sigma^3$
0.750	0.0028	0.820	0.00442	0.80429	0.0047	0.818
1.000	0.0281	0.698	0.03188	0.68411	0.0361	0.6894
1.150	0.076	0.606	0.08600	0.59138	0.0957	0.5761

Finally, we have also experimented with a different set of parameters for the two-body interactions. Now the Lennard-Jones parameters are determined via a self-consistent quantum-mechanical calculation [24] which yields a well depth ϵ/k =83 K and σ =3.350 Å. This, in turn, leads to $\nu/\epsilon\sigma^9 = 0.1202$. The coexistence curve for this *ab initio* model is plotted in Fig. 5. It is obvious from the figure that the use of potential parameters extracted from experimental results it is more appropriate.

IV. NO-SOLUTION BOUNDARIES IN THE RHNC EQUATION

The existence of a no-solution boundary for the integral equation is closely connected with the phase coexistence. The desirable situation would be to have a spinodal line delimiting the no-solution region. But unfortunately the RHNC equation behaves in a peculiar way.

The behavior of the integral equation in the vicinity of the no-solution region can be explored monitoring the isothermal compressibility χ_T along an isochore, when approaching the end point where the integral equation breaks down. In a pure spinodal behavior, χ_T should diverge to infinity according to a power law. This is not the case for the RHNC closure.

In previous works [15,16] the low-density behavior of the HNC equation (note that HNC and RHNC coincide at low densities) has been studied in detail. One of the leading conclusions of the analysis in Refs. [15] and [16] is that the low-density boundary of the no-solution region of the integral equation is not spinodal. Isochores end at the no-solution line in square-root branch points [16] where two solutions of the integral equation merge (one of then physically meaningful). The limiting behavior of the compressibility can then be fitted to an expression of the form [27]

$$\left(\frac{\rho\chi_T}{\beta}\right)^{-1} = b + a\sqrt{T - T_a} \tag{22}$$

with T_a being the temperature at the no-solution line. This sort of behavior has also been found by us here. This is illustrated in Fig. 6, which shows the fitting of the inverse isotherm compressibility to (22) at $\rho\sigma^3 = 0.1$. The results confirm that the present integral equation has the aforementioned singularity in the low-density region. This feature is inherent to the HNC and related integral equations whenever there is a possible phase separation [16].

In the high-density boundary, although the compressibility diverges to infinity, it also deviates from a spinodal behavior. In this regard Poll and Ashcroft [28] found a nonclassical divergence in the RHNC equation for a two-Yukawa fluid different from the power-law dependence.

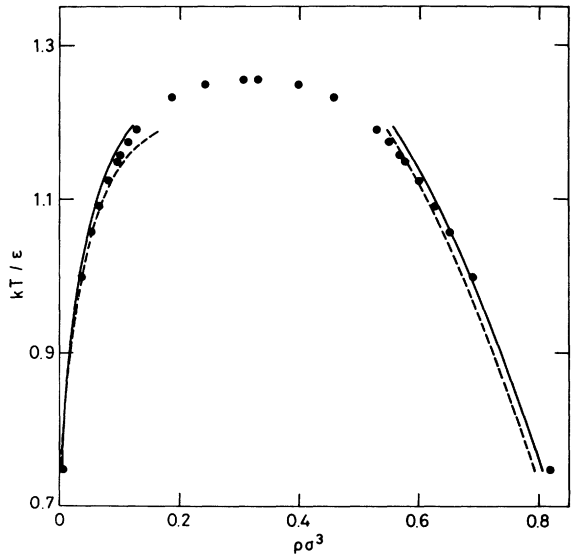

FIG. 5. Gas-liquid coexistence curve for two sets of LJ parameters for the LJ-Axilrod-Teller fluid (ϵ/k = 120 K, σ = 3.405 Å, solid line) and (ϵ/k = 83 K, σ = 3.350 Å, dashed line). Experimental data for argon are denoted by filled circles.

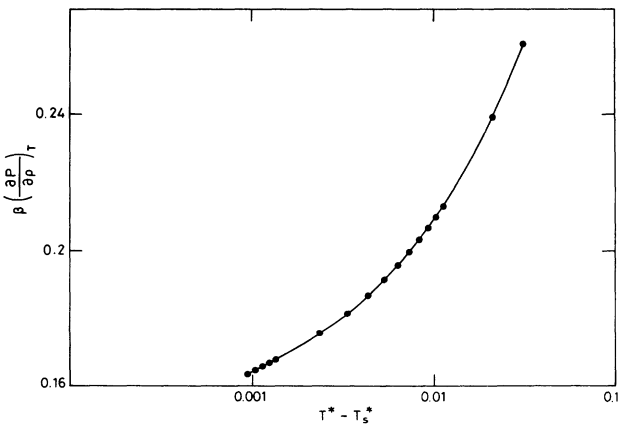

FIG. 6. Inverse isothermal compressibility close to the no-solution boundary at $\rho\sigma^3 = 0.1$. Solid circles represent the values rendered by the integral equation and the line denotes a nonlinear fit of Eq. (22).

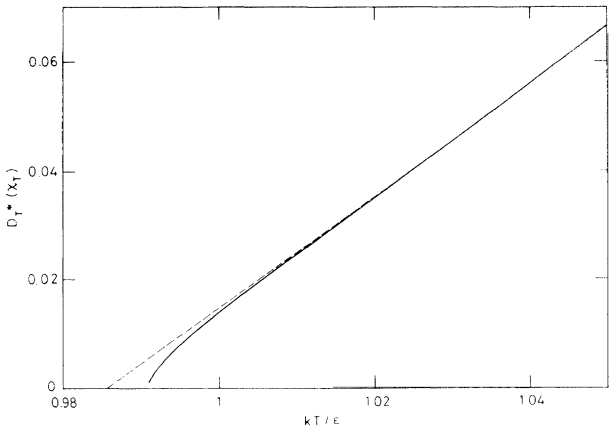

FIG. 7. $D_T(\chi_T)$ vs kT/ϵ [see Eq. (23) in the text]. The dashed line would represent a spinodal power-law divergence.

By monitoring the function

$$D_T(\chi_T) = \left(\frac{d[\ln(1/\chi_T)]}{dT}\right)^{-1} \tag{23}$$

along an isochore one finds that if the variation of χ_T is spinodal (i.e., $\chi_T \sim [(T - T_a)/T_a]^{-\gamma}$), $D_T(\chi_T)$ should be linear in T near T_a. Figure 7 shows a plot of $D_T(\chi_T)$ vs T in the present problem for an isochore evaluated at $\rho\sigma^3 = 0.5$. The behavior is similar to that found by Poll and Ashcroft [28] and we may say that also here a nonclassical divergence takes place.

We can then conclude that a main drawback of the RHNC approach in relation with the treatment of phase coexistence problems is the inability of the integral equation to render results in a region of considerable extent around the critical temperature. This is a pathological feature of the RHNC (and HNC) which is absent in other integral equations such us the mean spherical approximation (MSA). This suggests that a combination of the MSA long-range behavior and a term that corrects the poor performance of this approximation close to the particle core (such as using a hard-sphere fluid bridge function) would provide an alternative to bypass the deficiencies inherent to HNC-like approximations. This idea essentially constitutes the so-called crossover integral equation (CRS), proposed by Foiles, Ashcroft, and Reatto [14]. In a parallel work we have investigated this approximation for the pairwise Lennard-Jones system [13], and the no-solution line of this equation is shown in Fig. 8 together with coexistence curve for the LJ fluid from computer simulation and in the RHNC approximation. Here it can be appreciated that the no-solution line for the CRS equation lies always inside the coexistence curve. Moreover, the maximum of the no-solution line is found in the neighborhood of the simulated critical point. The boundary is produced by a spinodal divergence both at low and high density in accordance with the findings of

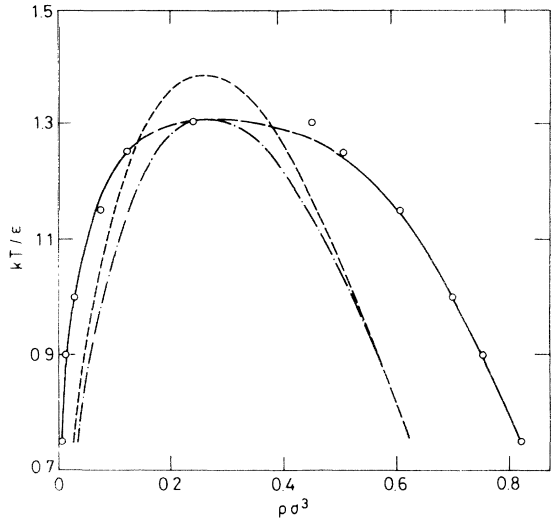

FIG. 8. Gas-liquid phase-coexistence curve for the 6-12 LJ fluid computed from the RHNC equation (solid line) and Gibbs ensemble simulation from Ref. [26] (open circles). The dashed line indicates the no-solution line of the RHNC equation, and the dot-dashed line indicates the no-solution line of the CRS equation.

Poll and Ashcroft [28], who encountered a typical power-law divergence with MSA critical exponents. It is not surprising that for low densities this approximation is free from the square-root branch points that affect the HNC equation. One must bear in mind, in this regard, that the bridge function vanishes with density as ρ^2, so the MSA contribution becomes the drawing force as far as the spinodal decomposition is concerned. However, one should not expect the MSA component to be able to capture the important association and clustering effects that can be found for low densities and strong attractive interactions [29].

A major shortcoming of the CRS approximation is the lack of a closed expression to compute free energies or chemical potentials. This problem might be solved at low densities or above the critical temperature by standard thermodynamic integration, but on the liquid side of the spinodal boundary there is no alternative route, and therefore, unfortunately the CRS integral equation is not yet a viable approach to determine the coexistence curve.

ACKNOWLEDGMENTS

We acknowledge the Centro Técnico de Informática del CSIC and very especially the Centro de Supercomputación de Galicia (CESGA) for generous access to their computing facilities. This research was financially supported by the Spanish Dirección General de Investigación Científica y Técnica (DGICYT) under Grant No. PB91-0110.

[1] M. V. Bobetic and J. A. Barker, Phys. Rev. B **2**, 4169 (1970).
[2] J. A. Barker, R. A. Fisher, and R. O. Watts, Mol. Phys. **21**, 657 (1971).
[3] J. A. Barker and M. L. Klein, Phys. Rev. B **7**, 4707 (1973).
[4] J. A. Barker, Phys. Rev. Lett. **57**, 230 (1986).
[5] B. M. Axilrod and E. Teller, J. Chem. Phys. **11**, 299 (1943).
[6] P. Attard, Phys. Rev. A **45**, 5649 (1992).
[7] P. Attard, Phys. Rev. A **45**, 3659 (1992).
[8] G. S. Rushbrooke and M. Silbert, Mol. Phys. **12**, 505 (1967).
[9] G. Casanova, R. J. Dulla, D. A. Jonah, J. S. Rowlinson, and G. Saville, Mol. Phys. **18**, 589 (1970).
[10] F. Lado, S. M. Foiles, and N. W. Ashcroft, Phys. Rev. A **28**, 2374 (1983).
[11] J. P. Hansen and L. Verlet, Phys. Rev. **184**, 151 (1969).
[12] R. D. Weir, I. WynnJones, J. S. Rowlinson, and G. Saville, Trans. Faraday Soc. **63**, 1320 (1967).
[13] E. Lomba and J.A. Anta (unpublished).
[14] S. M. Foiles, N. W. Ashcroft, and L. Reatto, J. Chem. Phys. **80**, 4441 (1984).
[15] J. S. Høye, E. Lomba, and G. Stell, Mol. Phys. **79**, 523 (1993).
[16] L. Belloni, J. Chem. Phys. **98**, 8080 (1993).
[17] J. P. Hansen and I. R. McDonald, *Theory of Simple Liquids* (Academic, London, 1990).
[18] S. Labík and A. Malijevský, Mol. Phys. **67**, 431 (1989).
[19] E. Lomba, Mol. Phys. **68**, 87 (1989).
[20] S. Labik, A. Malijevsky, and P. Vonka, Mol. Phys. **56**, 709 (1985).
[21] J. G. Kirkwood, J. Chem. Phys. **3**, 300 (1935).
[22] The original Kirkwood derivation is based on the assumption that the pair potentials of the mean force that can be evaluated in a triplet of particles add up to the three-body potential of mean force. If three-body potentials are present they have to be added as well and this accounts for the exponential term in Eq. (9).
[23] M. J. Gillan, Mol. Phys. **38**, 1781 (1979).
[24] G. C. Maitland, M. Rigby, E. B. Smith, and W. A. Wakeham, *Intermolecular Forces* (Clarendon, Oxford, 1981).
[25] A. Michels, J. M. Levelt, and W. De Graaff, Physica **24**, 659 (1958).
[26] A. Z. Panagiotopoulos, Mol. Phys. **61**, 813 (1987).
[27] F. Gallerani, G. Lo Vecchio, and L. Reatto, Phys. Rev. A **31**, 511 (1985); **32**, 2526 (1985).
[28] P. D. Poll and N. W. Ashcroft, Phys. Rev. A **32**, 1722 (1985).
[29] M. J. Gillan, Mol. Phys. **49**, 421 (1983).